



Automatic traffic monitoring by ϕ -OTDR data and Hough transform in a real-field environment

ESTER CATALANO, AGNESE COSCETTA, ENIS CERRI, NUNZIO CENNAMO, LUIGI ZENI, AND A. MINARDO*

Department of Engineering, Università della Campania Luigi Vanvitelli, Via Roma 29, 81031 Aversa, Italy

*Corresponding author: aldo.minardo@unicampania.it

Received 10 February 2021; revised 26 March 2021; accepted 5 April 2021; posted 7 April 2021 (Doc. ID 422385); published 21 April 2021

In this paper, we demonstrate automatic vehicle detection and counting by processing data acquired using a phase-sensitive optical time-domain reflectometer (ϕ -OTDR) distributed optical fiber sensor. The acquired data are processed using the Hough transform, which detects the lines in the images formed by representing the acquired data in the space–time domain. A rough classification of the vehicles (heavy versus light vehicles) is also proposed, based on the amplitude of the vibration data along the detected lines. The method has been experimentally tested by performing ϕ -OTDR measurements along a telecommunication fiber cable running in a buried conduit along the state road SS18 (province of Salerno, Italy), opened to normal traffic. Comparison with ground-truth data, manually generated by inspecting video recordings, allowed us to estimate a vehicle detection success rate up to 73%, while heavy vehicles were fully detected. © 2021 Optical Society of America

<https://doi.org/10.1364/AO.422385>

1. INTRODUCTION

Intelligent vehicle detection, counting, and classification are important tasks in the field of highway management. Traffic data may be obtained from different sensors installed along the road, such as loop detectors, ultrasonic sensors, or cameras. The use of video cameras (many of which are already installed to survey road networks), coupled with computer vision techniques is very effective, because the information contents associated with image sequences allows precise vehicle tracking and classification [1]. However, video cameras have high power consumption, and need a sufficient illumination for working properly. Furthermore, their operation can be negatively affected by weather conditions. Other common technologies are loop detectors, magnetic sensors (magnetometers), radar sensors, and microwave detectors. All these approaches have their merits and disadvantages, but usually they can detect the vehicle at only one position (where the sensor is placed), and therefore several of them must be deployed to monitor a road network.

Recently, distributed optical fiber vibration/acoustic sensors (DVS/DAS) based on the phase-sensitive optical time-domain reflectometry (ϕ -OTDR) have attracted a great deal of attention, thanks to their high sensitivity, long measurement range, high acquisition rate, and ease of installation (the optical fiber must be accessed from only one end). In conventional ϕ -OTDR systems, an optical pulse from a narrow-linewidth laser is injected into the fiber under test (FUT), and the backscattered light is collected to form a trace showing a random pattern

of Rayleigh backscattering. The random pattern remains the same if the external environment does not change; instead, when an external disturbance alters the refractive index of the fiber in some positions, a vibration signal can be extracted from the differences between successive traces in those positions. DVS/DAS sensors have been successfully applied in several fields, such pipeline monitoring [2], intrusion detection [3], and seismic monitoring [4]. In the transportation field, they have been employed in railway traffic monitoring [5,6]. Recently, roadway traffic monitoring based on DVS/DAS sensors has been reported as well [7–10]. When applied to road traffic monitoring, conventional optical fiber cables deployed for communication purposes and buried underground can be employed as sensors. Therefore, traffic monitoring can be realized at no additional installation cost, making use of otherwise dark telecommunication fibers. Previous reports indicate that the DVS/DAS technology is suitable for detecting and tracking vehicles, thanks to the vibrations transmitted underground by the seismic waves generated by vehicle passage. However, most results have been achieved in a controlled environment, or using manual (not automatic) vehicle counting. More recently, an automatic template-matching detection algorithm based on roadbed strain was applied to DAS measurements [11]. The results were found to be well correlated with mobile phone locations and urban seismic noise levels; however, no ground-truth data was available to calculate the actual detection success rate.

In this paper, we propose and demonstrate the use of a feature extraction technique usually employed to identify a certain class of shapes in images, the Hough transform (HT), for automatic

detection of vehicle passage based on ϕ -OTDR measurements. While the HT can more generally identify positions of arbitrary shapes, including circles and ellipses, we refer here to the classical HT, i.e., the one concerned with the identification of lines in the image. The HT is very effective in dealing with imperfect instances of an object, such as the case of the traces impressed by the vehicle passages in ϕ -OTDR measurements. Under constant speed condition, the vehicle signature is a linear segment, which is detected by the HT. The reported tests have been carried out in conditions of normal traffic. Differently from the template-matching algorithm employed in [11], the method described here utilizes the distributed nature of ϕ -OTDR data (i.e., data are processed in the spatiotemporal domain [12]). Furthermore, the results of automatic vehicle counting have been validated against ground-truth data provided by a camera. A threshold method is also proposed to distinguish between light and heavy vehicles. In practice, we show that the amplitude of the ϕ -OTDR data is correlated to the vehicle class, therefore a simple thresholding method can be used to distinguish between light and heavy vehicles.

2. SENSOR CONFIGURATION

Distributed acoustic measurements were carried out using a custom prototype, implementing the ϕ -OTDR configuration shown in Fig. 1. Light from an external cavity laser emitting at 1550 nm, with a linewidth of 10 kHz and an output power of 15 dBm, is pulsed through an electro-optic intensity modulator and then amplified through an erbium-doped fiber amplifier (EDFA). The amplified pulses are sent to the FUT through an optical circulator. The backscatter light is first amplified by another EDFA, and then sent to a narrowband (0.04 nm) fiber Bragg grating, centered at the laser wavelength, in order to filter out the amplified spontaneous emission noise of the EDFA placed in the detection path. Finally, the light is converted to an electrical signal through a photodetector connected to a fast digitizer. The digitizer board is equipped with a field-programmable gate array for real-time averaging of the acquired waveforms. The signal acquired by the setup is the intensity of the Rayleigh scattering excited by the injected pulses and has a typical speckle appearance. When a vibration impinges on the fiber in some point, the relative change in the local refractive

index modifies the amplitude (and phase) of the Rayleigh scattering signal generated by the probe pulse across the vibrating region. In general, the amplitude of the backscatter signal in a specific point is not a linear (nor monotone) function of the applied vibration. Therefore, amplitude-based configurations cannot provide quantitative measurements. However, they have been used successfully for detecting and even classifying disturbance events, for example, in security applications and intrusion detection of pipelines [3,13].

The FUT chosen for the measurements was a standard G-652 fiber accessible through the data center of Connectivia facilities (Angri, Italy). Connectivia is a wireless and wired (FTTH) Internet Service Provider, specialized in the field of wireless broadband connectivity. The fiber was running into a 6.4-mm polyethylene-coated, non-armored cable with four stranded loose-tubes. Each loose-tube was gel-filled and included 12 fibers with 250- μ m acrylate jacket. The FUT was \approx 900 m long, part of which (i.e., from $z \approx$ 150 m to $z \approx$ 900 m) was running under the two-lane, two-way state road SS18, at a depth of about 40 cm under the road surface and at a position nearly correspondent to the middle of one lane (see Fig. 2). The fiber departs from the Connectivia building, and runs in three sectors: first, from north to south along \approx 150 m (sector 1); then, from west to east along \approx 50 m (sector 2); and lastly, from east to west along \approx 700 (sector 3).

The fiber cable, installed inside the duct pipe using the air blowing method, was used in the past for digital communication between two offices. At the present, the cable is no longer used for communication, but it is still accessible through the data center.

When a vehicle circulates above the buried fiber, some vibration is generated and propagates through the ground, reaching the optical fiber running along the duct. These vibrations are detected by the DVS equipment, which therefore is able to detect and track the vehicle. However, some processing is required in order to distinguish the signals produced by the vehicle passage from noise. In the following section, the various processing steps will be described, together with the procedure adopted for automatic road traffic monitoring.

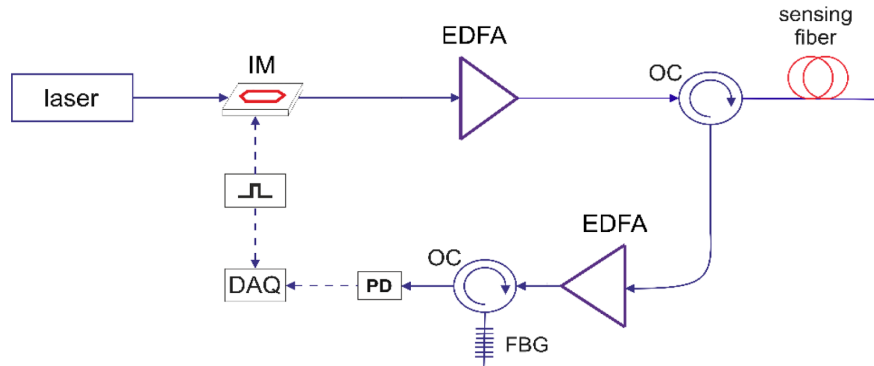


Fig. 1. ϕ -OTDR setup employed for road traffic monitoring. IM, intensity modulator; OC, optical circulator; EDFA, erbium-doped fiber amplifier; FBG, fiber Bragg grating; PD, photoreceiver; DAQ, data acquisition.



Fig. 2. View of the optical fiber path. The red marker indicates the location of the Connectivia building (Immagini @2021 Maxar Technologies, Dati cartografici @2021).

3. SIGNAL PROCESSING

The DVS prototype implementing the scheme in Fig. 1 has been employed to record continuously the backscatter traces along the FUT. The measurements were taken adopting a duration of the probe pulse equal to 50 ns, corresponding to a spatial resolution of ≈ 5 m. Pulse duration was chosen based on the necessity to distinguish consecutive vehicles, while ensuring at the same time an adequate signal-to-noise ratio (SNR). The pulse repetition rate was set to 80 kHz, while the number of averages was 1024. The resulting acquisition rate was ≈ 78 waveforms/s, which resulted in a vibration bandwidth of 39 Hz according to Nyquist's theorem. This was considered sufficient for the detection of the vibration noise generated by vehicle passages [9]. The acquired waveforms were grouped in frames, each one containing $p = 2344$ consecutive waveforms, corresponding to 30 s of continuous recording. The sampling step chosen for waveform sampling was 156 MS/s, corresponding to a sampling step of 64 cm along the FUT. As the FUT length was 900 m, this corresponded to $m = 1406$ sampling points. Therefore, each frame consisted in a $p - \text{by} - m$ matrix. Data in each frame were preprocessed according to the following steps:

- A matrix of size $(p - 1) - \text{by} - m$, whose elements were the differences between the rows of the frame matrix, was calculated to enhance the difference between consecutive waveforms, while removing the common parts.
- The absolute value operator was applied to the matrix obtained in step (a).

- A detrend operator was applied to each row of the matrix obtained in step (b), in order to remove dc offset, as well as any linear trend from the acquired waveforms.
- A moving average filter was applied to each column of the matrix obtained in step (c), using a lowpass filter with filter coefficients equal to the reciprocal of the span. The number of data points for calculating the smoothed values was set to 21, corresponding to a temporal span of 270 ms.
- A moving average filter was applied to each row of the matrix obtained in step (d), using a lowpass filter with filter coefficients equal to the reciprocal of the span. The number of data points for calculating the smoothed values was set to 5, corresponding to a spatial span of 3.2 m.
- A normalization procedure was applied by dividing each row of the matrix obtained in step (e) by its 2-norm.

All calculations were done in real time by a PC interfaced with the digitizer board through a PCIe interface, under MATLAB environment. As an example, we compare in Fig. 3 the originally acquired data, with the image obtained following the steps from (a) to (f). We note that two lines are discretely visible in the processed matrix, revealing the passage of two vehicles in the selected frame at a speed of ≈ 14 and 10 m/s, respectively.

For a sufficiently short spatial interval, a constant speed for the vehicles passing over that interval can be assumed. In this case, the vibration will appear as a line segment in the selected frame. A proper image processing algorithm, therefore, can be applied to detect automatically the vehicles passing over that

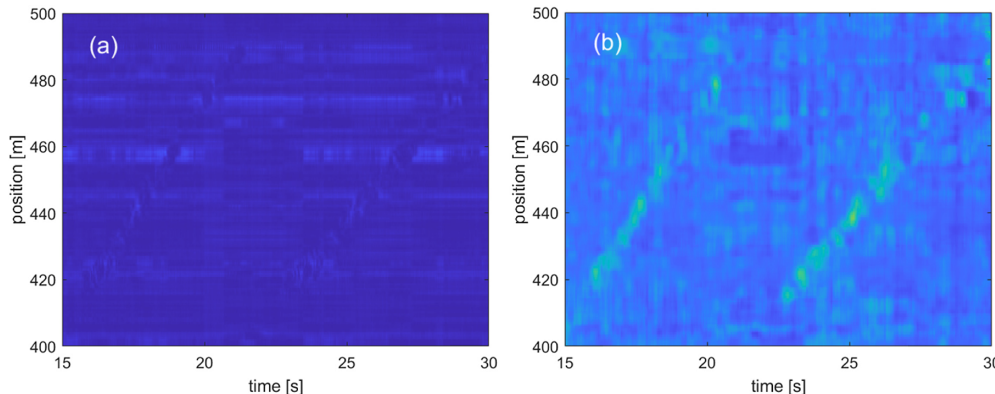


Fig. 3. Example image of (a) raw and (b) preprocessed DVS recording showing the traces of two vehicles.

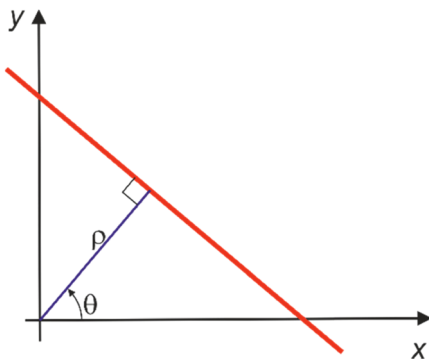


Fig. 4. Graphical representation of the Hough coordinates (ρ, θ).

region. The standard Hough transform is a widespread method for detecting lines or portions of lines in an image [14]. The HT transforms a binary image in a parameter space matrix in the (ρ, θ) domain, where each (ρ, θ) pair represents a line according to the following parametric representation:

$$\rho = x \cos \theta + y \sin \theta. \quad (1)$$

The first parameter ρ is the distance from the origin of the closest point of the line, while θ is the angle of the perpendicular projection from the origin to the line, measured in degrees clockwise from the positive x axis (see Fig. 4).

In order to calculate the HT, a 2D array known as an accumulator, whose size is equal to the number of possible (quantized) values of ρ and θ , is initialized to zero. For each point (x, y) of the analyzed image, if a pixel “1” exists in that point, the HT calculates the ρ coordinate of the line passing for that point for any possible θ . Thus, the corresponding accumulator cells (ρ, θ) are incremented. After all points in the analyzed image have been analyzed, each cell in the accumulator matrix represents the number of points lying along the corresponding (ρ, θ) line. Therefore, the largest matrix elements correspond to lines that have the largest number of points in the xy plane. In order to determine the position and the length of these lines, a further processing of the image is required. The HT method is tolerant with respect to defects and noise in the image. Therefore, even lines with missing points can be detected. This is essential in our application, as the lines generated by the passage of vehicles in the ϕ -OTDR data are strongly affected by noise, fading, and imperfect positioning of the buried fiber. Another important aspect is the calibration of the parameters chosen for line detection. In fact, a minimum length of the lines detected by the HT is generally set to avoid false detections. In our tests, this length was set to 45 pixels. Another parameter is the gap, i.e., the distance between two-line segments associated with the same HT bin: when the distance between the line segments is less than the specified value, the line segments are merged into a single line segment. In our tests this value was set to 10 pixels. In order to minimize the number of false positives, a further constraint was set in our analysis, dealing with the range of θ coordinate in the Hough plane chosen for the line search. In fact, the θ parameter is directly connected to the vehicles' speed. Limiting the vehicle speed in the range of 10–100 km/h, the range of possible θ coordinates for HT computation was determined. Finally, we have considered only vehicles traveling in one direction (i.e.,

only negative angles in the HT domain). This is justified by the fact that, while measurements were done in a two-lane, two-way road, the duct with the FUT was buried in the middle of one of two lanes (the one running from east to west). Thus, vibrations coming from vehicles passing over the opposite lane were much weaker and have been discarded in our analysis.

4. EXPERIMENTAL RESULTS

The results reported in this section have been obtained by analyzing the subset of DVS recordings relative to the interval 160–190 m. For such a short range, we can safely assume a constant vehicle speed, and therefore a linear trace in the space–time image plane. The choice of that particular interval came from the observation that the quality of the lines (i.e., the SNR of the acquired data) impressed by the vehicle transits on that interval was better than elsewhere. The HT was then applied to each 30-s frame, in order to detect the vehicle passages. Note that an image binarization was required before HT calculation. This was done using the Otsu's method, which chooses the threshold to minimize the intraclass variance of the black and white pixels [15]. In Fig. 5 we show an example of application of the HT for line detection in one of the acquired frames. We note that the slope of the lines in Fig. 5 is opposite to the one in Fig. 3. This is due to the fact that, in the portion considered in Fig. 5 (sector 2), the fiber ran in opposite direction with respect to the portion shown in Fig. 2 (sector 3).

In order to determine the capabilities of the sensor to monitor the traffic flow for a determined road segment, the DVS signal was acquired for 60 min. During acquisitions, the road length chosen for the HT was also monitored through video recording. The video was analyzed off-line, in order to determine the number of vehicle passages over the lane corresponding to the buried duct, for each 10-min time frame. Figure 6 compares the actual passages and the HT-determined passages during each frame. We see that the detected passages are a fraction of the actual ones, with an overall detection success rate of 73% (456 detected passages out of 623). While a different choice of the HT parameters (e.g., minimum length of the detected lines) may increase this percentage, this would also lead to the occurrence of false positives. Instead, with the chosen parameters we did not experience

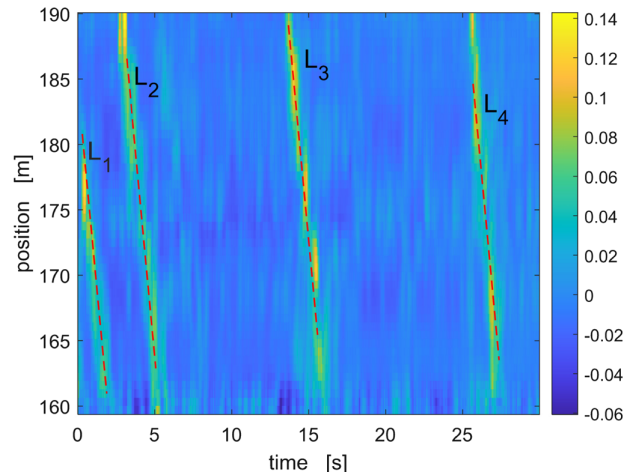


Fig. 5. Preprocessed DVS recordings superimposed to the lines detected by the HT.

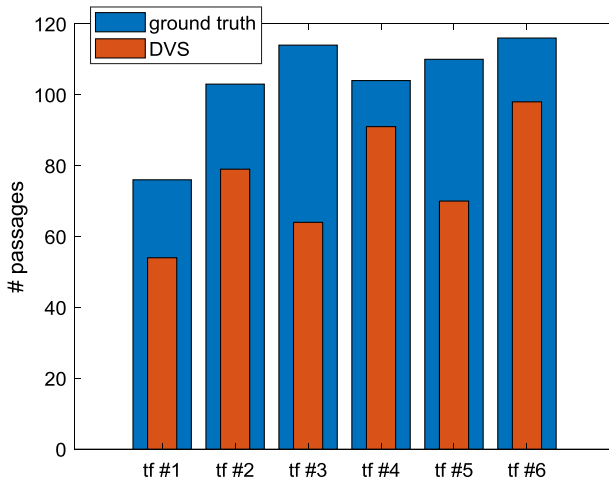


Fig. 6. Number of actual (blue bars) and HT-detected (red bars) vehicle passages, for each time frame of 10 min.

any false positives. We also note that a manual counting of the lines in the acquired images may provide a higher detection rate. However, the primary objective of this paper is to demonstrate the use of an automatic detection method. We believe that the detection rate in our tests was mostly limited by the SNR of measurements, rather than by the detection algorithm. In other words, the trace impressed by the passage of vehicles (especially the lighter ones), was too close to noise to be detected by the HT in 27% of the cases. The use of an optimized DVS sensor, a better positioning of the FUT, or a more efficient preprocessing of the acquired data [9], may significantly improve the success rate [10].

A further analysis of the acquired data was carried out in order to determine the capability of the system to discriminate between “light” vehicles and “heavy” vehicles. In this case, vehicles are classified as “heavy” or “light” based on the number of axles, with heavy vehicles being the ones with five or more axles. This choice is motivated by the fact that no weighing system was available for the monitored road, while the number of axles for each vehicle could be easily extracted from the videos. For this analysis, the maximum amplitude of the DVS signal over each detected line was taken as an indicator of the vehicle class. In fact, analyzing the videos we have found that a certain degree of correlation exists between the vehicle class and the DVS signal amplitude. In particular, we have found that a threshold of 0.145 for the maximum amplitude was suitable to discriminate between light and heavy vehicles (let us remind that the processed data were normalized according to the procedure described in Section 2). As an example, we show in Fig. 7 an acquired frame, together with the detected lines labeled with their corresponding maximum signal amplitude. We see that, out of five detected lines, only one reaches an amplitude larger than the set threshold. The analysis of the video record actually revealed the passage of a heavy truck in correspondence of that line.

In Fig. 8, the results obtained by analyzing the DVS data are compared to the ones obtained from video analysis. We see that the number of heavy vehicles detected by processing the DVS signal is larger than the actual value (32 detected passages against 29 actual ones). Analyzing the video, we have verified

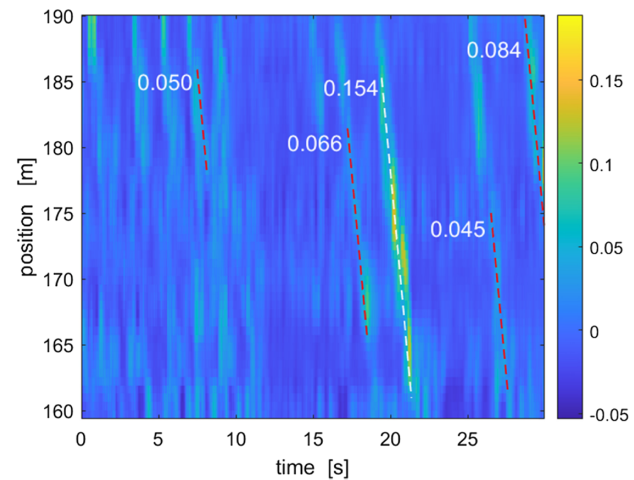


Fig. 7. Preprocessed DVS recordings superimposed to the lines detected by the HT, and with indication of the maximum amplitude of the acquired data along each line.

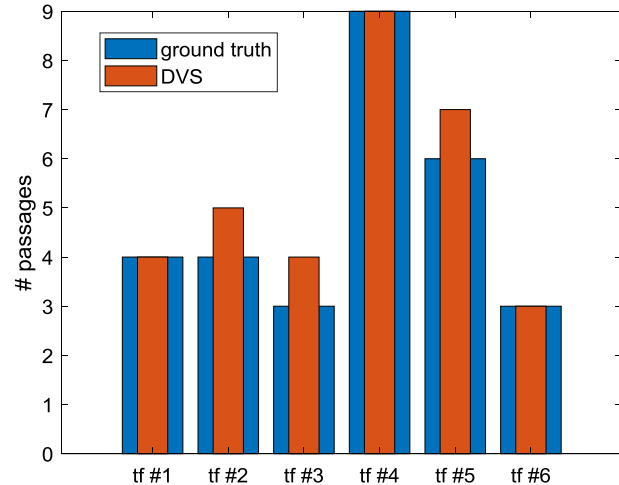


Fig. 8. Number of actual (blue bars) and HT-detected (red bars) heavy vehicle passages, for each time frame of 10 min.

that the 32 detected passages include all the 29 vehicles with five or more axles, with the addition of three “special” vehicles (a tanker and two tarpaulin vans). Probably, these vehicles had a weight comparable to trucks with five or more axles, giving rise to a comparable vibration amplitude. Unfortunately, no weigh-in-motion system was available during the tests to confirm this hypothesis.

5. CONCLUSIONS

A method for automatically processing the data acquired using a ϕ -OTDR sensor has been described. The method makes use of the Hough transform to detect lines in the images that represent the data acquired by the distributed sensor in space and time. Comparison with ground-truth data in a field trial permitted us to quantify the effectiveness of the proposed methodology. Furthermore, a certain degree of correlation between the amplitude of the vibration data and the class of the

vehicle has been found, showing that heavy trucks can be recognized from ϕ -OTDR data by setting a proper threshold. The present work demonstrates that the optical fiber infrastructure already available for data transmission can be used to perform traffic monitoring activities, at no additional installation cost. Furthermore, the proposed automatic detection method may be equally employed in case of DAS sensors with phase retrieval (such as the one employed in [11]), with the further advantage that in that case more sophisticated algorithms can be combined with the one proposed here for vehicle localization and classification [16,17].

Funding. POR FESR CAMPANIA 2014/2020 (B43D1800029007, Quick&Smart).

Acknowledgment. We thank Connectivia for their continuous support and for giving us access to their FFTH infrastructure.

Disclosures. The authors declare no conflicts of interest.

Data Availability. Data underlying the results presented in this paper are not publicly available at this time but may be obtained from the authors upon reasonable request.

REFERENCES

1. J. Zhou, D. Gao, and D. Zhang, "Moving vehicle detection for automatic traffic monitoring," *IEEE Trans. Veh. Technol.* **56**, 51–59 (2007).
2. C. Wang, M. Olson, B. Sherman, N. Dorjkhant, J. Mehr, and S. Singh, "Reliable leak detection in pipelines using integrated DdTS temperature and DAS acoustic fiber-optic sensor," in *International Carnahan Conference on Security Technology (ICCS7)*, Montreal, Quebec, 2018, pp. 1–5.
3. F. Peng, H. Wu, X. H. Jia, Y. J. Rao, Z. N. Wang, and Z. P. Peng, "Ultra-long high-sensitivity Φ -OTDR for high spatial resolution intrusion detection of pipelines," *Opt. Express* **22**, 13804–13810 (2014).
4. S. Dou, N. Lindsey, A. M. Wagner, T. M. Daley, B. Freifeld, M. Robertson, J. Peterson, C. Ulrich, E. R. Martin, and J. B. Ajo-Franklin, "Distributed acoustic sensing for seismic monitoring of the near surface: a traffic-noise interferometry case study," *Sci. Rep.* **7**, 11620 (2017).
5. F. Peng, N. Duan, Y. J. Rao, and J. Li, "Real-time position and speed monitoring of trains using phase-sensitive OTDR," *IEEE Photonics Technol. Lett.* **26**, 2055–2057 (2014).
6. C. Wiesmeyr, M. Litzenberger, M. Waser, A. Papp, H. Garn, G. Neunteufel, and H. Döller, "Real-time train tracking from distributed acoustic sensing data," *Appl. Sci.* **10**, 448 (2020).
7. Z. Wang, Z. Pan, Q. Ye, B. Lu, Z. Fang, H. Cai, and R. Qu, "Novel distributed passive vehicle tracking technology using phase sensitive optical time domain reflectometer," *Chin Opt. Lett.* **13**, 100603 (2015).
8. H. F. Wang, D. Fratta, C. Lancelle, E. M. Ak, and N. E. Lord, "Distributed acoustic sensing (DAS) array near a highway for traffic monitoring and near-surface shear-wave velocity profiles," in *American Geophysical Union, Fall Meeting 2017, abstract #S33B-0866* (2017).
9. H. Liu, J. Ma, W. Yan, W. Liu, X. Zhang, and C. Li, "Traffic flow detection using distributed fiber optic acoustic sensing," *IEEE Access* **6**, 68968–68980 (2018).
10. G. A. Wellbrock, T. J. Xia, M. F. Huang, Y. Chen, M. Salemi, Y. K. Huang, P. Ji, E. Ip, and T. Wang, "First field trial of sensing vehicle speed, density, and road conditions by using fiber carrying high speed data," in *Optical Fiber Communications Conference and Exhibition (OFC)*, San Diego, California, 2019, pp. 1–3.
11. N. J. Lindsey, S. Yuan, A. Lelouch, L. Gualtieri, T. Lecocq, and B. Biondi, "City-scale dark fiber DAS measurements of infrastructure use during the COVID-19 pandemic," *Geophys. Res. Lett.* **47**, e2020GL089931 (2020).
12. H. F. Martins, M. R. Fernández-Ruiz, L. Costa, E. Williams, Z. Zhan, S. Martin-Lopez, and M. Gonzalez-Herraez, "Monitoring of remote seismic events in metropolitan area fibers using distributed acoustic sensing (DAS) and spatio-temporal signal processing," in *Optical Fiber Communications Conference and Exhibition (OFC)*, San Diego, California, IEEE, 2019, pp. 1–3.
13. H. F. Taylor and C. E. Lee, "Apparatus and method for fiber optic intrusion sensing," U.S. patent 5,194,847 (16 March 1993).
14. R. O. Duda and P. E. Hart, "Use of the Hough transformation to detect lines and curves in pictures," *Commun. ACM* **15**, 11–15 (1972).
15. N. Otsu, "A threshold selection method from gray-level histograms," *IEEE Trans. Syst. Man Cybern.* **9**, 62–66 (1979).
16. N. Shpalensky, L. Shiloh, H. Gabai, and A. Eyal, "Use of distributed acoustic sensing for Doppler tracking of moving sources," *Opt. Express* **26**, 17690–17696 (2018).
17. L. Jiajing, W. Zhao Yong, L. Bin, W. Xiao, L. Luchuan, Y. Qing, Q. Ronghui, and C. Haiwen, "Distributed acoustic sensing for 2D and 3D acoustic source localization," *Opt. Lett.* **44**, 1690–1693 (2019).